Experiments with Cloud Properties: Impact on Surface Radiative Fluxes

H. Wang[1], R. T. Pinker[1], P. Minnis[2], and M. M. Khaiyer[3]

1. Department of Atmospheric and Oceanic Science, University of Maryland, College Park, MD, 20742
2. MS 420, NASA Langley Research Center, Hampton, VA 23681-0001
3. Science Systems and Applications, Inc., Hampton, VA 23666

December 3, 2007

Accepted for Publication in

Journal of Atmospheric and Oceanic Technology

Abstract

Solar radiation reaching the Earth's surface provides the primary forcing of the climate system and thus, information on this parameter is needed at global scale. Several satellite based estimates of surface radiative fluxes are available but they differ from each other in many aspects. The focus of this study is to highlight one aspect of such differences, namely, the way satellite observed radiances are used to derive information on cloud optical properties and the impact this has on derived parameters such as surface radiative fluxes. Frequently, satellite visible radiance in a single channel is used to infer cloud transmission; at times, several spectral channels are utilized to derive cloud optical properties and use these to infer cloud transmission. In this study, an evaluation of these two approaches will be performed in terms of impact on the accuracy in surface radiative fluxes. The University of Maryland Satellite Radiation Budget model (UMD/SRB) is used as a tool to perform such an evaluation over the central United States. The estimated shortwave fluxes are evaluated against ground observations at the Atmospheric Radiation Measurement (ARM) Central Facility and at four ARM extended sites. It is shown that the largest differences between these two approaches occur during the winter season when snow is on the ground.

1. Introduction

Solar radiation incident at the earth surface determines the surface temperature, sensible and latent heat fluxes that govern most of dynamical and hydrological processes (Stephens and Greenwald, 1991). It plays an essential role in controlling biological processes (Running et al., 1999; Platt, 1986) and is also needed for validating climate models (Garrat et al., 1993; Wild et al., 1995; Wielicki et al., 2002). Clouds strongly interact with solar and terrestrial radiation and thus modulate the energy balance of the earth and the atmosphere as estimated from satellites (Ramanathan, 1987; Ramanathan et al., 1989) and from numerical models (Ramanathan et al., 1983; Cess et al., 1989). The largest uncertainties in surface short-wave flux estimates from satellites are due to inadequate information on cloud properties. There have been many attempts at both regional and global scales, to estimate surface radiative fluxes from satellite-observed radiances (Ramanathan, 1986; Pinker and Lazlo, 1992; Li and Leighton, 1993; Stephens et al., 1994; Gupta et al., 1999; Mueller et al., 2004; Raschke et al., 1991; Rigollier et al., 2004; Whitlock et al., 1995; Lefevre et al., 2007). Most models have been designed for use with a particular satellite, and frequently, cloud optical properties are inferred from a single visible channel. The use of multi-channel information is expected to provide more accurate description of cloud optical properties and subsequently, lead to improved estimates of surface solar fluxes. In this study, the effect of cloud optical properties as derived by two independent methods (single channel and a two-channel approach) on the estimation of surface shortwave fluxes is evaluated. The UMD/SRB model is used as a tool to perform such an evaluation. The original version of the model (Model A) utilizes the visible channel (0.52-0.72 am) of GOES satellites to infer cloud optical depth. The National Aeronautics and Space Administration (NASA) Langley Cloud and Radiation Research Group derives cloud optical depth over the ARM Southern Great Plains (SGP) region from multiple channels of GOES. To use such information directly in the UMD/SRB model, it is necessary to redesign Model A. The modified version will be labeled Model B. The independently derived cloud properties provided by the NASA Langley group (Minnis et al., 2002) over the ARM SGP site will be used to drive this version of the inference scheme. The resulting surface short-wave fluxes from both versions are compared with ground observation at the ARM Central Facility, as well as at four extended ARM sites. In section 2 Models A and B are described. Data used are discussed in section 3. Results are presented in section 4 and a summary is presented in section 5.

2. Model Description

Model A is a physical inference scheme based on radiative transfer theory (Pinker et al., 2003). Using forward radiative transfer calculations, relationships are established between the broadband (0.2-4.0 μm) transmissivity and the reflectivity at the top of atmosphere under various conditions pertaining to surface, atmosphere, and clouds. The radiative fluxes at the surface and at the top of the atmosphere are computed by determining the atmospheric transmission and reflection and the surface albedo pertaining to a particular satellite observation. First, surface albedo is derived from satellite measured radiances at the TOA that represent average clear sky conditions. Once the surface albedo is determined, the atmospheric transmission and reflection (Optical Functions) for instantaneous clear and cloudy conditions are obtained by matching the broadband TOA albedos with those computed by the radiative transfer model. The retrieved optical functions, along with surface albedo are used to compute fluxes for clear and cloudy conditions. Finally, clear and cloudy fluxes weighted by the pixel number of clear and cloudy conditions are summed up to obtain all-sky fluxes.

In Model B, the need to first estimate surface albedo, aerosol and cloud properties from the clear or cloudy radiances is by-passed. Instead, information on cloud properties is imported from independent sources, in this case, the LaRC products. Additional input parameters on the state of the atmosphere needed to drive the model include aerosols, surface albedo, water vapor and ozone amount. To isolate the effect of independently derived cloud properties, all the other input parameters are kept the same as those used in Model A.

3. Data

The surface radiative fluxes used in the comparison were obtained from Version 2.1 of Model A (Li et al., 2007; Pinker et al., 2007) and from Model B driven with cloud information as obtained from the NASA Langley Cloud and Radiation Research Group.

Version 2.1 of Model A is based on an operational real time scheme (Version1.1) as used at the National Oceanic and Atmospheric Administration (NOAA)/National Environmental Satellite Data and Information Service (NESDIS) since January 1996, in support of the GEWEX Continental Scale International Project (GCIP). The primary observing system in these two versions is the visible channel (0.52-0.72 μm) on the GOES satellites, which is a narrow-band channel. The radiative fluxes are derived for 0.5^0 latitude/longitude grid cells. The 4 km pixels within a grid cell are classified into cloudy, mixed and clear pixels. Cloud fraction and mean TOA albedo of clear sky and cloudy sky are then calculated for the grid cell and provided to Model A to infer radiative fluxes. Instantaneous, hourly, daily, and monthly mean information on surface down-welling shortwave (SW), top of the atmosphere downward and upwelling radiative fluxes, are provided for an area bounded by 70^0-125^0 W longitude and 25^0-50^0 N latitude. Version 2.1 of Model A uses updated calibration of the visible sensor, an improved cloud detection scheme, in particular, better cloud detection over snow (Li et al., 2007; Pinker et al., 2007), and improved atmospheric input parameters such as ozone (which till now was taken from climatology).

The independently derived cloud properties used as inputs to Model B are based on the Visible-Infrared-Solar Infrared-Split Windows Technique (VISST), which is an update of Solar-Solar Infrared-Infrared method described by Minnis et al. (Minnis, 1995). Each GEOS 4km pixel is classified as clear or cloudy using a modified version of the cloud identification method (Trepte el al., 1999) developed for the Cloud and Earth's Radiant Energy System (CERES). Cloud properties of cloudy pixels are derived at half-hourly time scale from January 1 to December 31, 2000 using VISST and then averaged into 0.5^0 latitude/longitude cell boxes. The spatial coverage of the derived cloud properties extends from 32.25^0-41.75^0 N and 91.25^0-104.750 W.

Ground observations are taken from the Central Facility and four extended sites of ARM SGP at one minute intervals. For the Central Facility, the down-welling shortwave irradiance from the ARM Best Estimate (BE) Flux Value Added Product (VAP) is used. The BE Flux VAP uses data available from the three co-located radiometer platforms (Solar and Infrared Radiation Station (SIRS) C1, E13, and Baseline Solar Radiation Network (BSRN)) to determine the best available irradiance measurements (Shi and Long, 2002). For extended sites, the down-welling shortwave irradiance is from "sirs1butt" VAP which is SIRS measurements with the correction for infrared loss to the diffuse shortwave measurements (Long et al., 2001; Younkin and Long, 2003). To match the estimated surface downward short-wave fluxes at a resolution of half a degree, the one minute point measurements are averaged over a 30-minutes interval centered at the satellite observations.

4. Results

The ground sites are usually not located in the center of the 0.5^0 grid cells, and therefore, they do not necessarily represent the 0.5^0 grid cell average. Therefore, the estimated fluxes were interpolated into 0.5^0 grid cells centered at five ground sites using inverse distance weighting interpolation method. For each ground site, the measured down-welling shortwave irradiance was compare with estimate from the two models and bias, square root mean error and correlation coefficient were computed.

Table 1 shows the evaluation results for Model B at the central facility for the entire period of 2000. For most months, except for January and December, the correlation coefficient is larger than 0.96. RMSE ranges from 42 to 83 W/m^2, which is about 8 to 20% relative to the mean of the ground observations. The bias varies from -25 to 21 W/m^2 (relative value of 0.4-7%). However, for January and December, the difference between model estimates and ground measurements is relatively large, with correlation coefficients of 0.92 and 0.89, bias of -30 (11%) and -34 (13%) W/m^2 and RMSE of 77 (27%) and 83 (31) W/m^2, respectively

It is of interest to understand the relatively larger difference between model estimates and ground observations during the winter months. Figure 1 shows the daily average surface albedo at central facility for December and at Extended Site-1 for January. Surface albedo at Central Facility was provided by the BE Flux VAP. At Extended Site-1, downwelling and upwelling shortwave irradiances are used to calculate surface albedo. During these two months, one third of the days had a surface albedo greater than 0.4 indicating snow conditions. Figures 2 and 3 present the scatter plots of estimated fluxes from Model B against ground observations at the central facility for December and Extended Site-1 for January, respectively. The sample points in the scatter plot are classified into two groups. One consists of cases where surface albedos are less than 0.4 (marked by solid triangle), and the other with surface albedo greater than 0.4 (marked by circles). The two figures clearly show that Model B underestimates the surface downward shortwave fluxes when the surface albedo is greater than 0.4; the relatively low correlation coefficient, large negative bias and large RMSE seem to be related to the presence of snow at the surface. Tables 2 and 3 present the evaluation results of Models A and B for the two winter months. During December Model A flux estimates have a higher correlation coefficient, smaller rms error and bias when compared to ground observations at the Central Facility than those estimated by Model B. At Extended Site-1 for January, fluxes from the two models have the same correlation coefficient while Model A fluxes have a smaller bias and RMSE than Model B.

Figure 4 shows scatter-plots of estimated fluxes from Models A and B against ground observations at the Central Facility for 2000. The twelve months of 2000 are grouped as follows: DJF (December, January and February), MAM (March, April and May), JJA (June, July and August), and SON (September, October and November). For MAN, JJA and SON, the corresponding correlation coefficients for Model B are 0.97, 0.96, 0.97, with relative RMSE of 15, 14 and 13% and relative biases of 2, 3 and 2 %, while Model A results have correlation coefficients of 0.95, 0.94 and 0.96, relative RMSE of 18, 18, 14% and relative biases of 0.4, 2, 2%. For DJF, Model B correlation coefficient is 0.93, the relative bias is 10% and the relative RMSE is 22%. For Model A the correlation coefficient is 0.92, the relative bias is 5 % and the relative RMSE is 21%.

The satellite estimates at the four extended ARM sites are of similar accuracy as found at the Central Facility. During snow free periods Model B (ARM SGP VISST cloud product) is in better agreement with ground observations than Model A while the latter performs better during the winter season.

5. Summary

In recent years, progress has been made in the development and launch of multi-spectral Earth Observing Systems. Most current estimates of surface SW radiative fluxes are based on geostationary satellites that have the capability to capture the diurnal variation of clouds. Instruments onboard such satellites have coarse spectral and spatial resolution and thus, are limited in their capability to accurately detect cloud or/and aerosol optical properties that are important elements of the radiation budget. At the same time, these inference schemes have a tested infra-structure for assessing radiative fluxes. It is therefore of interest to evaluate the ability of these schemes to use independently derived optical parameters that can be obtained from dual or multi-channel observations. The evaluation performed in the present study utilizes cloud properties based on the UMD/SRB model that uses a single channel retrieval of cloud optical depth and a multi-spectral approach provided by the NASA Langley Cloud and Radiation Research Group over the Southern Great Plains. The multi-spectral approach is more complex than the single channel one and its applicability in real time is of issue. It is of interest to evaluate the impact of the multi-channel approach on estimating surface radiative fluxes. Such an evaluation has been undertaken in this study.

The advanced scheme of the NASA Langley Cloud and Radiation Research Group retrievals should in principle lead to more accurate cloud optical properties and a better estimate of surface shortwave fluxes than the simplified inference schemes. Over a one year period, cloud properties derived by this advanced scheme do yield better estimates of surface fluxes during snow free conditions. During the winter months when snow is on the ground Version 2.1 of Model A has lower RMSE and a smaller bias than Model B.

The study also demonstrates the ability of Model B to estimate surface fluxes with independent satellite based estimates of cloud optical properties. This is of interest since observations from multi-channel systems have the potential to improve estimates of cloud optical parameters. For example, the Moderate Resolution Imaging Spectro-radiometer (MODIS) instrument onboard the Terra and Aqua satellites is a state-of-the-art sensor with 36 spectral bands (King et al., 1992) with demonstrated capabilities to provides high quality cloud detection and to estimate optical properties of both aerosols and clouds (Kaufman et al., 1997; Platnik et al., 2003). Improvements in estimating surface shortwave fluxes are anticipated from the implementation of Model B with cloud and aerosol optical properties from new generation of satellite instruments of higher spectral and spatial resolution such as MODIS on Terra and Aqua or the Spinning Enhanced Visible and Infrared Imager (SEVIRI) on METEOSAT-8. Moreover, the evaluation presented here seems timely due to the upcoming A-train satellite constellation that consists of six sun synchronous satellites and carries advanced instruments that should provide improved information on clouds and aerosols (Stephens et al., 2002).

Acknowledgement

Support by NASA EOD/IDS grant NAG59634 and NASA grant NNG05GB35G to the University of Maryland is greatly appreciated. This research was also supported by the Atmospheric Radiation Measurement (ARM) Program sponsored by the U.S. Department of Energy (DOE), Office of Energy Research, Office of Health and

Environmental Research, Environmental Sciences Division under Interagency Agreement ITF No. 18971.

References:

Garrat, J. R., P. B. Krummel, and E. A. Kowalczyk, 1993. The surface energy balance at local and regional scales-A comparison of general circulation model results with Observations. *J. Climate, 6,* 1090-1109.

Gupta, S. K., N. A. Richey, A. C. Wilber, C. H. Whitlock, G. G. Gibson, and P. W. Stackhouse Jr., 1999. A climatology of surface radiation budget derived from satellite data. J. Climate, 12, 2691-2710.

Kaufman, Y. J., D. Tanré, L. Remer, E. F. Vermote, A. Chu, and B. N. Holben, 1997. Operational remote sensing of tropospheric aerosol over the land from EOS-MODIS, J. Geophys. Res., *102,* 17,051-17,068.

King, M. D., Kaufman, Y. J., Menzel, W. P., and Tanré, D., 1992. Remote sensing of cloud, aerosol, and water vapor properties from the Moderate Resolution Imaging Spectrometer (MODIS). IEEE Transactions on Geosciences and Remote Sensing, *30*, 2-27.

Lefèvre M., Diabaté L., Wald L., 2007. Using reduced data sets ISCCP-B2 from the Meteosat satellites to assess surface surface solar irradiance. Solar Energy, 81, 240-253, doi:10.1016/j.solener.2006.03.008.

Li, X., R. T. Pinker, M. M. Wonsick, and Yingtao Ma, 2006. Towards improved satellite estimates of short-wave radiative fluxes: Focus on cloud detection over snow. 1. Methodology: J. Geophys. Res., Vol. 112, No. D7D0720810.1029/2005JD006698

Li, Z., and H. G. Leighton, 1993. Global climatology of solar radiation budget at the surface and in the atmosphere from 5 years of ERBE data. J. Geophys. Res., 98, 4919-4930.

Long, C. N., K. Younkin, and D. M. Powell, 2001. Analysis of the Dutton et al. IR loss correction technique applied to ARM diffuse SW measurements. In *Proceedings of the Eleventh Atmospheric Radiation Measurement (ARM) Science Team Meeting*, ARM-CONF-2001. U.S. Department of Energy, Washington, D.C.

Lucht, W., C. B. Schaaf, and A. H. Strahler, 2000. An Algorithm for the Retrieval of Albedo from Space Using Semi-empirical BRDF Models. *I*EEE Trans. Geosci. Remote Sens., **38,** 977-998.

Minnis, P., Kratz, D. P., Coakley, J. A., Jr.; King, M. D., Garber, D., Heck, P., Mayor, S., Young, D. F., and Arduini, R., 1995. Cloud Optical Property Retrieval (Subsystem 4.3). Clouds and the Earth's Radiant Energy System (CERES) Algorithm Theoretical Basis Document, Volume III: Cloud Analyses and Radiance Inversions (Subsystem 4), *NASA RP 1376 Vol. 3*, edited by CERES Science Team, December, 1995, pp. 135-176.

Minnis, P., W. L. Smith, Jr., D. F. Young, L. Nguyen, A. D. Rapp, P. W. Heck, and M. M. Khaiyer, 2002: Near-real-time retrieval of cloud properties over the ARM CART area from GOES data. *Proc. 12th ARM Science Team Meeting, April 8-12, St. Petersburg, FL, 7 pp.*

Pinker, R.T. and I. Laszlo, 1992. Modeling surface solar irradiance for satellite applications on a global scale. J. Appl. Meteor., 31, 194-211.

Pinker, R. T., J. D. Tarpley, I. Laszlo, K. E. Mitchell, P. R. Houser, E. F. Wood, J. C. Schaake, A. Robock, D. Lohmann, B. A. Cosgrove, J. Sheffield, Q. Duan, L. Luo, and R. W. Higgins, 2003. Surface radiation budgets in support of the GEWEX Continental Scale International Project (GCIP) and the GEWEX Americas Prediction Project (GAPP), including the North American Land Data Assimilation System (NLDAS) project. J. Geophys. Res., 108 (D22), 8844, doi:10.1029/2002JD003301.

Platnick, S., M. D. King, S. A. Ackerman, W. P. Menzel, B. A. Baum, J. C. Riédi, and R. A. Frey, 2003. The MODIS Cloud Products: Algorithms and Examples from Terra. IEEE Trans. Geosci. Remote Sens., *41*, 459-473.

Platt, T., 1986. Primary production of the ocean water column as a function of surface light intensity: Algorithms for remote sensing. Deep Sea Res., 33, 149-163.

Pinker, R. T., Xu Li and Wen Meng, 2007. Towards improved satellite estimates of short-wave radiative fluxes: Focus on cloud detection over snow. Part II: Results. J. Geophys. Res., 112, D09204, doi:10.1029/2005JD006699.

Ramanathan, V., 1986. Scientific use of surface radiation budget data for climate studies. Surface Radiation Budget for Climate Application, J. T. Suttles and G. Ohring, Eds., NASA Reference Publication 1169, 58-86

Running, S. W., Collatz, G. J., Washburne, J., S. Sorooshian, 1999. Land Ecosystems and Hydrology. EOS Science Plan 5:197- 260.

Shi, Y., and C. N. Long, 2002. Best Estimate Radiation Flux Value Added Procedure: Algorithm Operational Details and Explanations. Atmospheric Radiation Measurement Program Technical Report, ARM-TR-008.

Stephens, G. L. and T. J. Greenwald, 1991. The earth's radiation budget and its relation to atmospheric hydrology, Part I: Observations of the clear sky greenhouse effect. J. Geophys. Res., 96, 15,311-15,324.

Stephens, G, L., A. Slingo, M. J. Webb, P. J. Minnett, P. H. Daum, L. Kleinman, I. Wittmeyer, and D. A. Randall, 1994. Observations of the earth's radiation budget in relation to atmospheric hydrology. 4: Atmospheric column radiative cooling over the world's oceans. J. Geophys. Res. 99, 18 585-18 604.

Stephens, G. L., D. G. Vane, R. J. Boain, G.G. Mace, K. Sassen, Z. Wang, A. J. Illingworth, E. J. O'Connor, W. B. Rossow, S. L. Durden, S. D. Miller, R. T. Austin, A. Benedetti, C. Mitrescu, and T. CloudSat Science Team, 2002. THE CLOUDSAT MISSION AND THE A-TRAIN. *B*ull. Amer. Meteor. Soc., 83, 1771–1790.

Trepte, Q., Y. Chen, S. Sun-Mack, P. Minnis, D. F. Young, B. A. Baum, and P. W. Heck, 1999. Proc. AMS 10th Conf. Atmos. Rad., Madison, WI, June 28-July 2, pp. 169-172.

Wielicki B. A, A. D. Del Genio, T. M. Wong, J. Y. Chen, B. E. Carlson, R. P. Allan, F. Robertson, H. Jacobowitz, A. Slingo, D. A. Randall, J. T. Kiehl, B. J. Soden, C. T. Gordon, A. J. Miller, S. K. Yang, J. Susskind, 2002. Changes in tropical clouds and radiation Response. Science, 296 (5576): U2-U3.

Wild, M., A. Ohmura, H. Gilgen, and E. Roeckner, 1995. Validation of GCM simulated radiative fluxes using surface observations. J. Climate, 8, 1309-1324.

Younkin, K. and Long, C. N., 2003. Improved Correction of IR Loss in Diffuse Shortwave Measurements: An ARM Value-Added Product (ARM-TR-009).

List of Figures

Table 1. Evaluation results of Model B for the entire period of 2000 at ARM Central Facility

Month of 2000	*Mean of Observation* *W/m^2*	*Bias* *W/m^2 (%)*	*RMSE* *W/m^2 (%)*	*Correlation Coefficient*	*Number of Observation*
Jan	286	-30 (11)	77 (27)	0.92	400
Feb	376	-25 (7)	59 (16)	0.97	446
Mar	356	-8 (2)	62 (17)	0.98	586
Apr	497	-11 (2)	72 (14)	0.97	621
May	512	-2 (1)	71 (14)	0.97	742
Jun	446	9 (2)	83 (19)	0.96	767
Jul	538	21 (4)	81 (15)	0.97	792
Aug	539	21 (4)	61 (11)	0.98	729
Sep	500	7 (2)	42 (8)	0.99	661
Oct	340	-24 (7)	69 (20)	0.97	577
Nov	289	-12 (4)	44 (15)	0.98	511
Dec	267	-34 (13)	83 (31)	0.89	444

Table 2. Comparison of evaluation results of Model A and Model B for December of 2000 at ARM Central Facility

Central Facility December	*Mean of Observation W/m^2*	*Bias W/m^2 (%)*	*RMSE W/m^2 (%)*	*Correlation Coefficient*	*Number of Observation*
Model A	314	-26 (8)	75 (24)	0.89	165
Model B	314	-46 (15)	101 (32)	0.83	165

Table 3. Comparison of evaluation results of Model A and Model B for January of 2000 at ARM Extended Site-1

Extended Site-1 January	*Mean of Observation W/m^2*	*Bias W/m^2*	*RMSE W/m^2*	*Correlation Coefficient*	*Number of Observation*
Model A	338	-27 (8)	92 (27)	0.77	125
Model B	338	-53 (16)	106 (31)	0.77	125

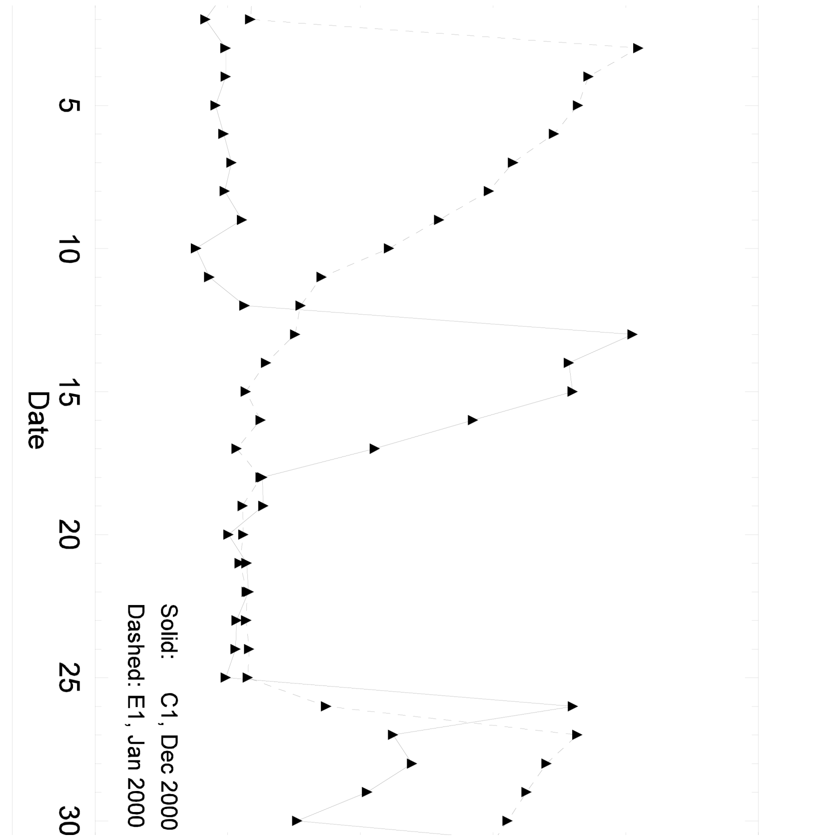

Figure 1 Daily average surface albedo for December of 2000 at the Central Facility and for January of 2000 at Extended Site-1.

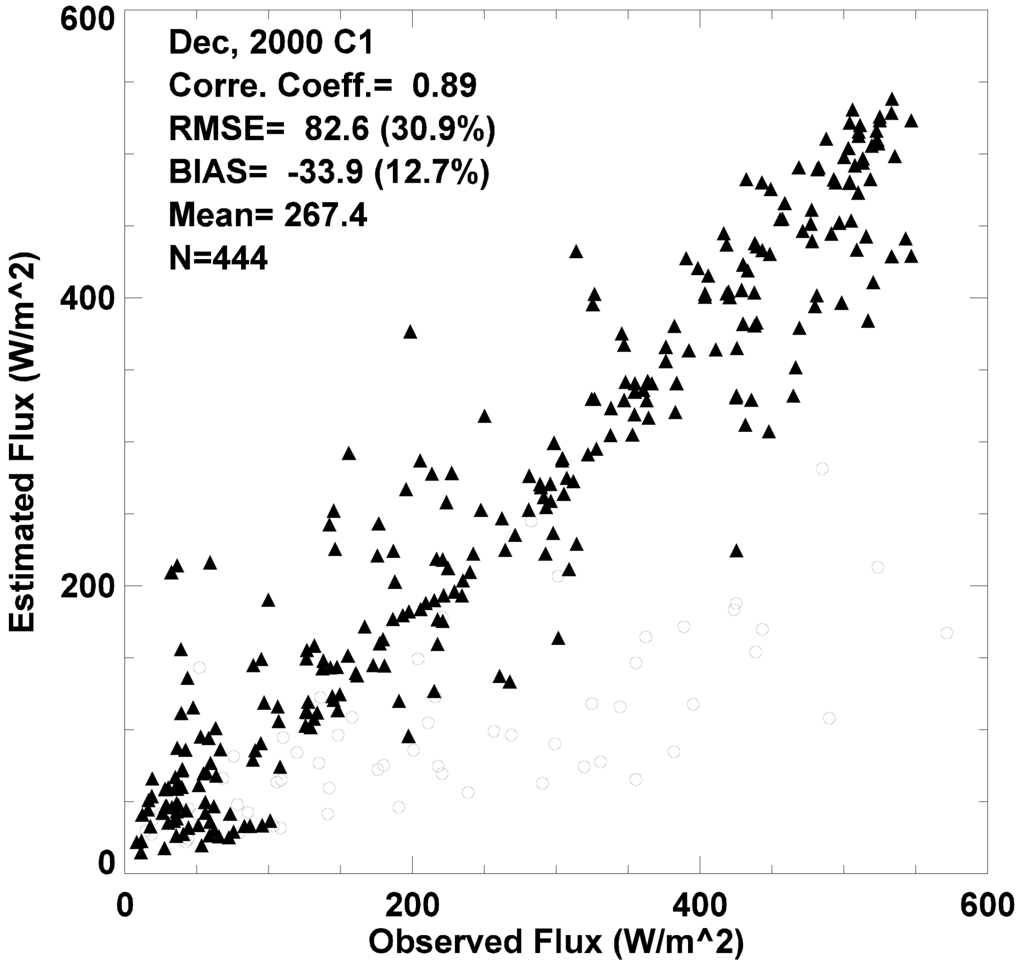

Figure 2. Validation of surface downward shortwave fluxes estimated with Model B driven with ARM SGP VISST cloud product against ground measurement at central facility of ARM for December of 2000.

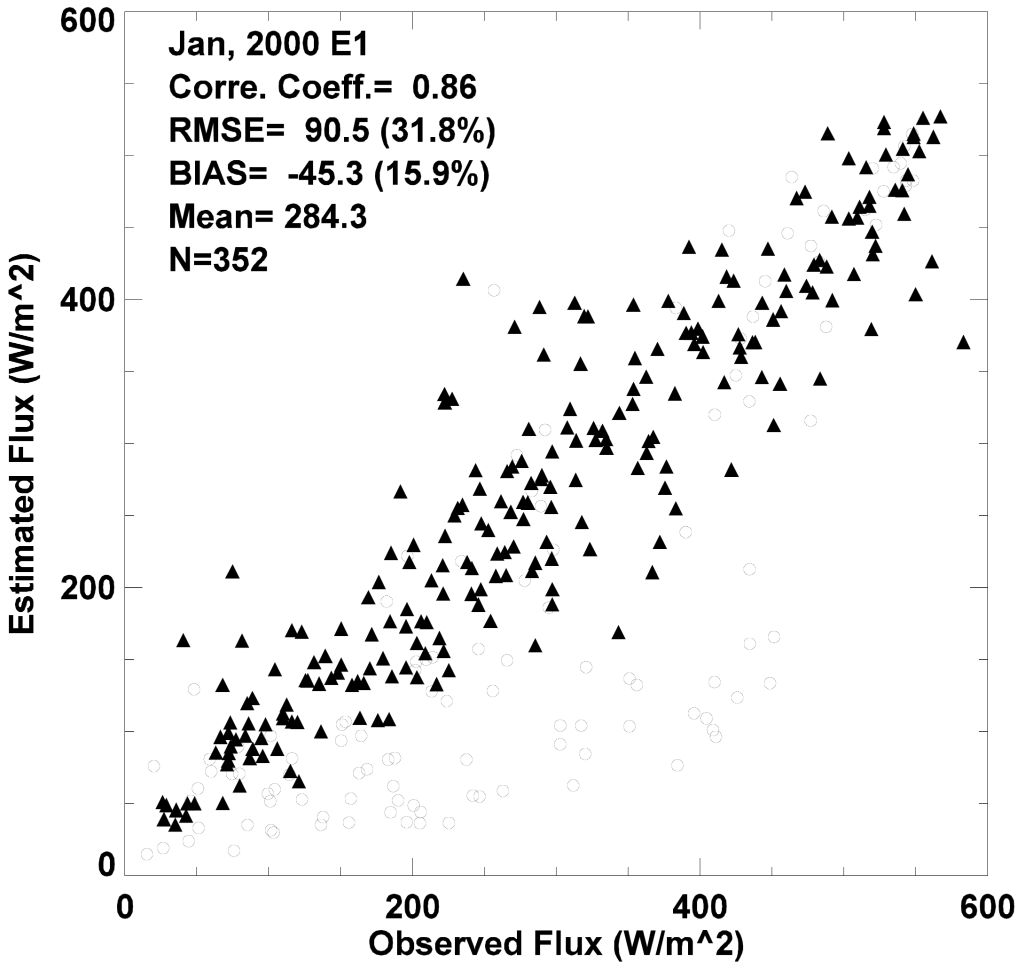

Figure 3. Validation of surface downward shortwave fluxes estimated with Model B driven with ARM SGP VISST cloud product against ground measurement at Extended Site 1 of ARM for January of 2000.

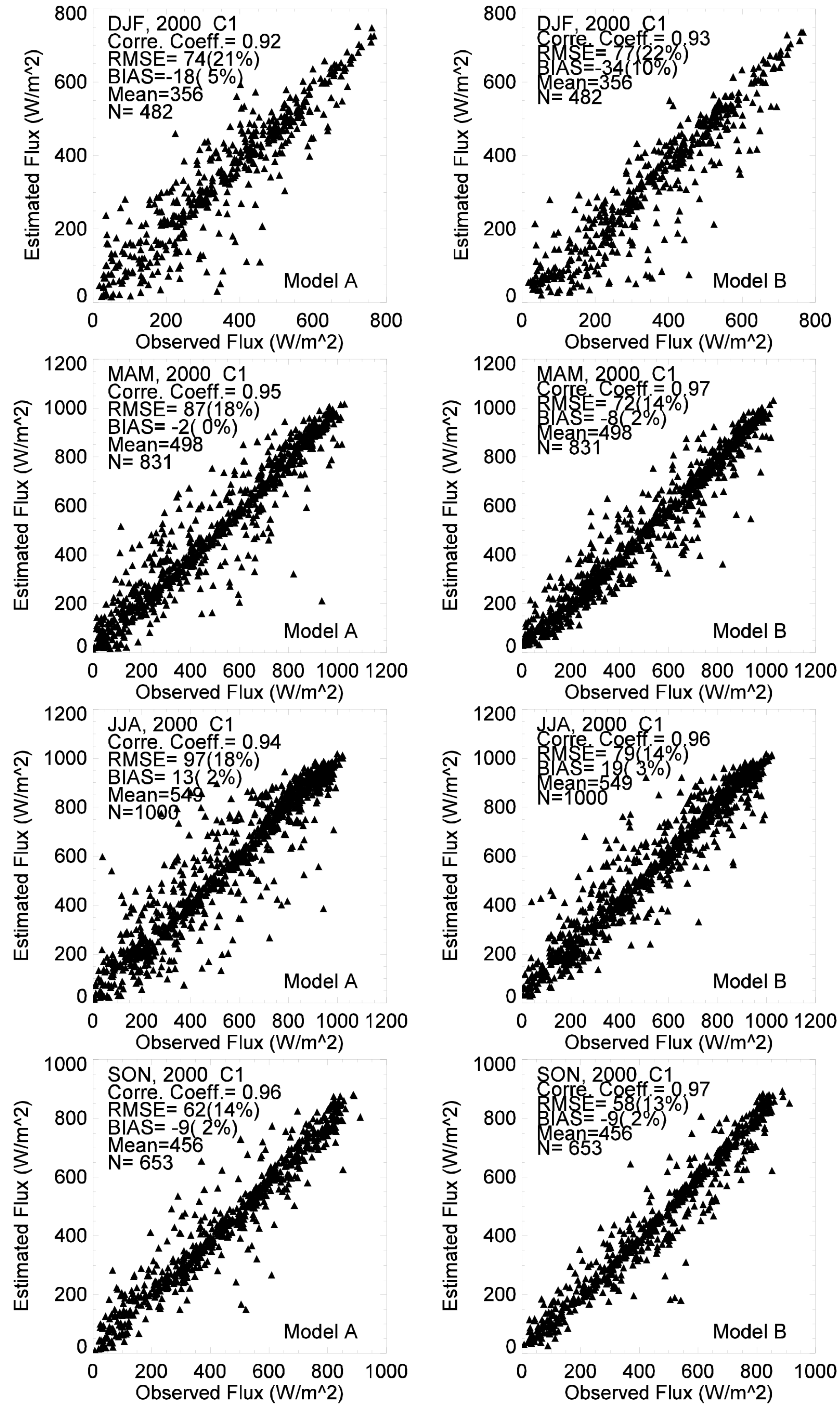
DJF, 2000 C1
Corre. Coeff.= 0.92
RMSE= 74(21%)
BIAS=-18(5%)
Mean=356
N= 482
Model A
DJF, 2000 C1
Corre. Coeff.= 0.93
RMSE= 77(22%)
BIAS=-34(10%)
Mean=356
N= 482
Model B
MAM, 2000 C1
Corre. Coeff.= 0.95
RMSE= 87(18%)
BIAS= -2(0%)
Mean=498
N= 831
Model A
MAM, 2000 C1
Corre. Coeff.= 0.97
RMSE= 72(14%)
BIAS= -8(2%)
Mean=498
N= 831
Model B
JJA, 2000 C1
Corre. Coeff.= 0.94
RMSE= 97(18%)
BIAS= 13(2%)
Mean=549
N=1000
Model A
JJA, 2000 C1
Corre. Coeff.= 0.96
RMSE= 79(14%)
BIAS= 19(3%)
Mean=549
N=1000
Model B
SON, 2000 C1
Corre. Coeff.= 0.96
RMSE= 62(14%)
BIAS= -9(2%)
Mean=456
N= 653
Model A
SON, 2000 C1
Corre. Coeff.= 0.97
RMSE= 58(13%)
BIAS= -9(2%)
Mean=456
N= 653
Model B
Estimated Flux (W/m^2)
Observed Flux (W/m^2)

Figure 4. Validation of surface downward shortwave fluxes derived by Model A and estimated by Model B driven with ARM SGP VISST cloud product against ground measurement at central facility of ARM for 2000.